Effect of geometric properties on temperature-dependent thermal conductivity of crud layer deposited in simulated PWR primary water

Hye Min Park[a,b], Hee-Sang Shim[a,*], Iseul Ryu[a], Young-Kook Lee[b], Do Haeng Hur[a]

[a]*Nuclear Materials Research Division., KAERI, 989-111 Daedeok-daero, Yuseong-gu, Daejeon 34057, Korea.*
[b]*Department of Advanced Materials Engineering, Yonsei University, 50 Yonsei-ro, Seodaemun-gu, Seoul 03722, Korea.*
[*]*Corresponding author: hshim@kaeri.re.kr*

1. Introduction

The amount of corrosion product deposits on fuel assemblies has recently been increased in many pressurized water reactors (PWRs) due to economic operating strategies of nuclear power plants such as power uprate, lifetime extension and higher burnup [1,2]. These deposits are called as 'crud' and are formed by corrosion products released from the surfaces of the reactor coolant system. It is well known that crud has a porous structure because crud deposition is stimulated in a condition where sub-cooled nucleate boiling ℃ curs [3]. Crud has a major concern in fuel reliability and reactor operation, including its safety under accident conditions. The crud disposed from PWR fuel rods consists mainly of a nonstoichiometric spinel $Ni_xFe_{3-x}O_4(0 \leq x \leq 1.0)$ with a small quantity of NiO, Fe_3O_4, ZrO_2 or Ni_2FeBO_5 [4-6]. Concentrated boron-containing compounds in the porous crud have induced l℃ al power distortion owing to neutron capture by boron and accelerated cladding corrosion due to reduction of heat transfer from fuel to coolant [3].

Understanding mechanism through which the crud conducts heat transfer over various power ranges of the nuclear fuel rods is very significant to predicting the fuel integrity. It is because the crud has a significantly lower thermal conductivity than the fuel cladding and it depends on characteristics of crud such as geometry and chemical composition. Thus, many researchers have studied the effect of crud properties on heat transfer of nuclear fuel. However, most of the studies were concentrated on modeling and simulation, and a few researchers have experimentally studied heat transfer properties of crud.

The crud obtained from nuclear power plant have shown a various porosity of 20~80% and the vicinity in crud layer have shown tortuous geometry [3,7]. However, the simplified and assume information is used to simulation and modelling of crud thermal property to evaluate core integrity [8-10]. Thus, the experimental data, which reflect the characteristics of real crud, are demanded to improve the uncertainty of simulation results.

In this work, dense and porous nonstoichiometric nickel ferrite ($Ni_xFe_{3-x}O_4$) cruds were deposited using vacuum sputtering system and simulated PWR primary loop, respectively. The physicochemical and thermal properties of cruds were analyzed by various analyzing equipment such as SEM, XRD, DSC, LFA, etc. From these data, we analyzed the relationship between crud characteristic and crud heat transport.

2. Experimental

In order to compare the effect of porosity on the thermal properties of crud deposited on the zirconium alloy fuel cladding surface, dense and porous cruds were prepared using vacuum sputtering system and simulated PWR primary loop, respectively. A zirconium alloy plates having same chemical composition with commercial Zirlo^{TM} cladding, which is summarized in Table I, were used as a substrate. The dimension of plate specimen is 10 mm x 10 mm x 0.48 mm (thickness). Prior to crud deposition, the specimen is cleaned with ultrasonication in acetone, alcohol and deionized water for each 10 min.

Table I. Chemical composition of Zr-alloy specimen (wt. %).

Sn	Fe	O	Nb	Zr
1.0	0.1	0.1	1.0	Bal.

Dense crud was deposited using a radio-frequency (RF) magnetron sputtering system to fabricate same composition with that deposited in simulated PWR primary coolant loop. The base pressure and working pressure were 5×10^{-7} and 5×10^{-3} Torr, respectively. Sputtering was performed using both NiO and Fe_3O_4 targets under argon gas at 300℃ for 112 h. Then, the RF power of NiO and Fe_3O_4 targets was controlled to 100 W and 400 W, respectively. The dense crud was deposited to be a thickness of 50 μm.

Porous cruds with different porosity were prepared using the simulated PWR primary coolant loop as shown in Fig. 1. The plate specimen was mounted on internal heater surface and it was inserted into the test section. The primary water was prepared by dissolving LiOH of 2 ppm and H_3BO_3 of 1,000 ppm into deionized water. The dissolved oxygen was controlled to be less than 5 ppb and dissolved hydrogen was maintained at 35 cc/kg·H_2O. The primary water was circulated with flow rate of 100 cc/min. The crud source was prepared by dissolving 600 ppm of nickel ethylenediamine tetraaccetic acid (EDTA) and 800 ppm of iron acetate into deionized water. The crud source solution was supplied to the test section at an injection rate of 1.0 cc/min, when the coolant temperature and pressure in test section was stabilized at 328℃ and at 12.8 MPa, respectively. The surface temperature of Zr-alloy plate

was maintained at 350℃ and 355℃, respectively, in order to control the porosity of crud. Then, the heat flux was calculated with 6.1 W/cm^2 and 6.8 W/cm^2 at the surface temperature of 350℃ and 355℃, respectively. The crud deposition was performed for 25 days.

The surface morphology of cruds deposited on fuel cladding material were observed using a scanning electron microscope (SEM). The cross-sectional images of cruds were obtained using SEM equipped with a f℃ used ion beam (FIB) to evaluate the porosity and thickness of cruds. Crystallinity of cruds were analyzed using X-ray diffraction (XRD). Thermal conductivity *(λ)* of cruds were obtained by multiplying the thermal diffusivity (*α*), specific heat capacity (c_p), and density *(ρ)*. These parameters were measured using laser flash analyzer (LFA), differential scanning calorimetry (DSC), and He gas pycnometer, respectively. The two-layer method was applied to analyze the thermal diffusivity of crud deposited on Zr-alloy specimens.

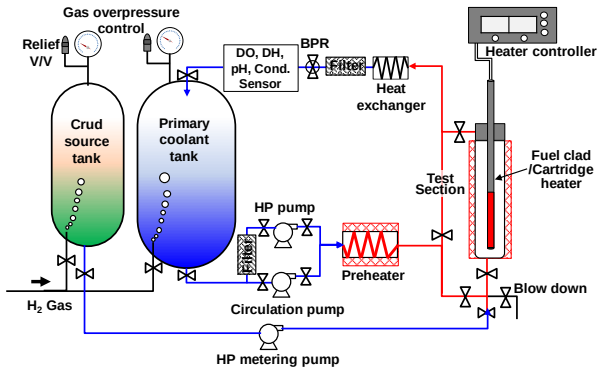

Fig. 1. A Schematic of the simulated crud deposition loop

3. Results and Discussion

Fig. 2 shows the SEM surface micrographs of dense and porous cruds. The surface of dense crud fabricated using sputter is very clean and smooth as shown in Fig. 2(a). However, many protruding structures and various size pores were observed in both specimen surfaces prepared using PWR primary coolant loop as shown in Figs. 2(b)-2(d). The surface of crud deposited at the surface temperature of 345℃ ($T_{surf.}$=345℃) and 350℃ ($T_{surf.}$=350℃) appeared rougher than that deposited at 355℃ ($T_{surf.}$=355℃) due to dendrite-shaped structures growing toward the coolant. This result indicates that the surfaces at two temperature conditions have experienced different boiling conditions.

Fig. 3 shows the cross-sectional SEM images of cruds fabricated using sputter and crud deposition loop. To analyze the cross-sectional images of cruds, the specimens were prepared by splitting the crud sputter-deposited on silicon wafer and by focused ion beam machining for cruds deposited in PWR primary coolant loop, respectively. The sputter-deposited crud shows dense film as shown in Fig. 3(a), although it displays slightly rough due to its preparation manner. However, both cruds deposited in PWR primary loop shows different thickness for the location and porous structure as shown in Fig. 3(b) and 3(c). Fig. 3(d) shows the average thickness and the porosity of three crud layers. The average thickness was 50 μm, 52 μm, 58.4 μm for each sputtered-deposited crud, crud for $T_{surf.}$=350℃ and that for $T_{surf.}$=355℃, respectively. The average porosity was measured by 0% for sputter-deposited crud, 27.4% for crud deposited at $T_{surf.}$=350℃, and 33.8% for crud deposited at $T_{surf.}$=355℃, respectively.

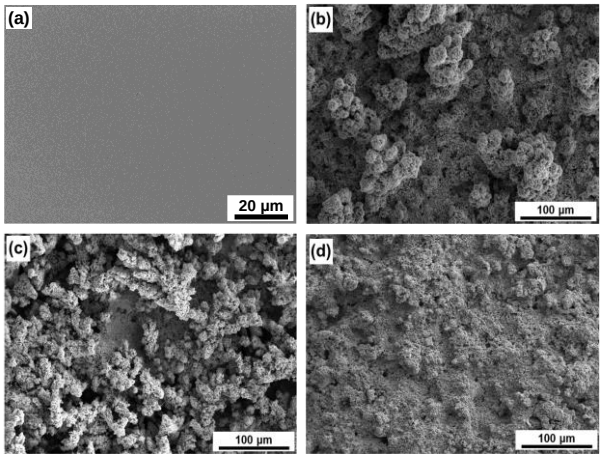

Fig. 2. SEM surface micrographs of (a) dense crud and porous cruds deposited in simulated primary coolant loop at the specimen surface temperature of (b) 345℃, (c) 350℃ and (d) 355℃.

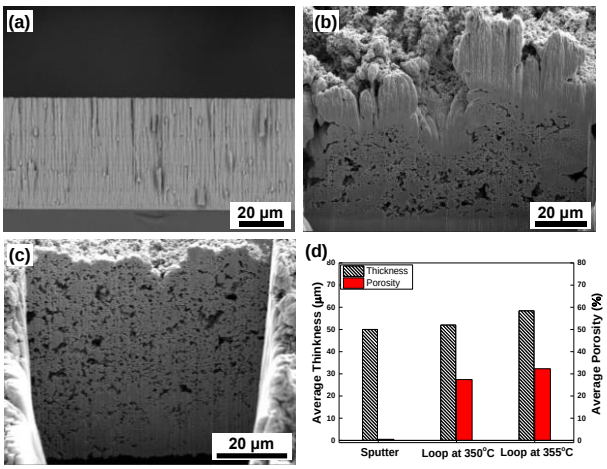

Fig. 3. SEM Cross-sectional micrographs of (a) dense cruds and porous cruds deposited at (b) 350℃ and (c) 355℃, and (d) information for average thickness and porosity.

To investigate the crystallinity of three cruds, the X-ray diffraction analysis was performed and the result were shown in Fig. 4. Three crud layers displayed a non-stoichiometric nickel ferrite ($Ni_xFe_{3-x}O_4$) and the characteristic peaks of XRD patterns for those cruds were consistent with the standard pattern of cubic spinel $Ni_{0.6}Fe_{2.4}O_4$ (JCPDS Card No. 87-2338). The Miller indices for the peaks were determined by using the relation between Sin 2θ values and the combined equation of the Bragg law with the plane-spacing equation for each crystal system. As denoted in the

figure, the Bragg planes such as (220), (311), (222), (400), (422), (511), (440), and (620) belong to the cubic spinel structure of the Fd-3 m space group. The most intense peak was observed on the (311) plane and no other separate peaks were identified by XRD.

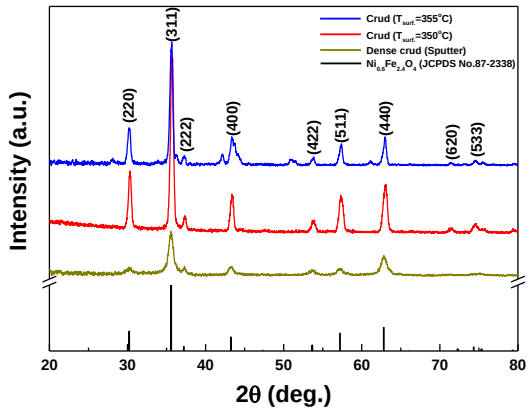

Fig. 4 XRD patterns of dense and porous cruds deposited on zirconium alloy plate.

To evaluate the effect of crud porosity on heat transport through it from zirconium alloy cladding surface, the thermal conductivity of crud was measured using LFA, DSC and He-pycnometer in the temperature range of 200~850℃ , as shown in Fig. 5. Then, the zirconium dioxide thickness was enough thin to be negligible in evaluation of thermal conductivity. The thermal conductivity of metallic zirconium alloy as a substrate material appears similar value with about 12 W/m·K in the temperature range of 200-600℃ but abruptly increases at the temperature range of 600-850℃ . However, the thermal conductivity of cruds deposited using simulated PWR primary coolant loop was lower with 0.46-1.53 W/m·K than that of zirconium metal alloy. The thermal conductivity of crud deposited at $T_{surf.}$=350℃, in which many dendrite structures were observed, was 0.46 W/m·K at 200℃ but it gradually increased up to 0.84 W/m·K at 850℃ with increase of specimen temperature.

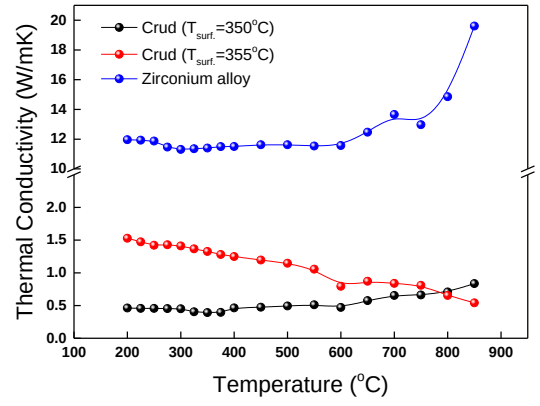

Fig. 5 Thermal conductivity of crud deposited on zirconium alloy specimen with different porosity in the temperature range from 200℃ to 850℃ .

However, thermal conductivity of crud deposited at $T_{surf.}$=355℃, which had higher porosity than that deposited at $T_{surf.}$=350℃ , was 1.53 W/m·K at 200℃ but gradually decreased with increase of specimen temperature. In addition, thermal conductivity of crud deposited $T_{surf.}$=355℃ become lower than that of crud deposited at $T_{surf.}$=350℃ at 800℃ . In general, it is well known that the thermal conductivity of ceramic materials decreases with increase of specimen temperature like that of crud deposited at $T_{surf.}$=355℃ [11]. However, the thermal conductivity of crud deposited at $T_{surf.}$=350℃ tends to increase as a function of specimen temperature and becomes higher than that of crud deposited at $T_{surf.}$=355℃ at 800℃ .

This result is considered to be because the crud structure is collapsed in high temperature during LFA analysis as shown in Fig. 6. An exposed location of substrate was observed in some areas after LFA analysis as not shown here. Therefore, thermal conductivity of crud deposited at $T_{surf.}$=350ºC would be affected by increase of substrate temperature due to its geometric change [12].

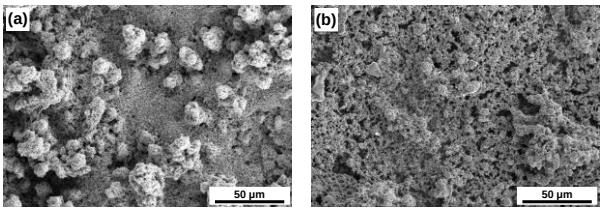

Fig. 6 Crud surface morphology (a) before and (b) after LFA analysis.

4. Conclusions

We have investigated the porosity effect of cruds deposited using sputtering and simulated primary coolant loop on its heat transport in this work. All crud layer is a non-stoichiometric spinel nickel ferrite ($Ni_{0.6}Fe_{2.4}O_4$) in XRD observation. The porosity of crud was higher in crud deposited at $T_{surf.}$=355℃ with 32.3% than that of crud deposited at $T_{surf.}$=350℃ with 27.4%. Thermal conductivity of crud was affected by both porosity and surface morphology. It might be because the thermal conductivity of crud is multiply affected by other properties such as surface structure and its thermal stability as well as its porosity. Therefore, it indicates that various geometry parameters of crud is considered together with the porosity to understand well the heat transport of crud at high temperature.

Acknowledgments

This work was financially supported by the National Research Foundation of Korea (NRF) grant funded by the government of the Republic of Korea (2017M2A8A4015159).

REFERENCES

[1] J. Deshon, D. Hyssey, B. Kedrick, J. McGurk, J. Secker, and M. Short, Pressurized Water Reactor Fuel crud and corrosion modeling Nuclear Reactor Power Monitoring, Journal of Materials, 2011
[2] G. Wang, W.A. Byers, M.Y. Young, J. Deshon, Z. Karpitas, and R.L. Oelrich, Thermal conductivity measurements for simulated PWR crud, International Conference on Nuclear Engineering, 2013
[3] J. Deshon, PWR Axial Offset Anomaly (AOA) Guidelines, Rev. 1, EPRI Report, 1008102, EPRI, Palo Alto, 2004.
[4] S. Odar, Crud in PWR/VVER coolant, A.N. T. Int'l, Sweden, 2014.
[5] J.-W. Yeon, I.-K. Choi, K.-K. Park, H.-M. Kwon, K. Song, Chemical analysis of fuel crud obtained from Korean nuclear power plants, J. Nucl. Mater. Vol.404, pp.160-164, 2010.
[6] J. A. Sawicki, Evidence of Ni_2FeBO_5 and m-ZrO_2 precipitates in fuel rod deposits in AOA-affected high boiling duty PWR core, J. Nucl. Mater. Vol.374, pp. 248-269, 2008.
[7] D. Hussey, D. Wells, Simulated Fuel Deposits Under PWR Zinc Chemistry Conditions, EPRI Report, 3002002891, EPRI, Palo Alto, 2017.
[8] M. P. Short, D. Hussey, B. K. Kendrick, T. M. Besmann, C. R. Stanek, S. Yip, Multiphysics modeling of porous CRUD deposits in nuclear reactors, J. Nucl. Mater. Vol.443, pp. 579-587, 2013.
[9] I. Haq, N. Cinosi, M. Bluck, G. Hewitt, S. Walker, Modelling heat transfer and dissolved species concentrations within PWR crud, Nucl. Eng. Des. Vol.241, pp. 155-162, 2011.
[10] J. Lee, H. Jeong, Y. Bang, Thermal resistance effects of crud and oxide layers to the safety analysis, Top Fuel, 2018.
[11] D. S. Smith, et al., Thermal conductivity of porous materials, J. Mater. Res., Vol.28, pp.2260-2272
[12] A. F. Renteria, B. Saruhan, U. Schulz, H.-J. Raetzer-Scheibe, J. Hang, A. Wiedenmann, Effect of morphology on thermal conductivity of EB-PVD PYSZ TBCs, Surf. Coat. Technol. Vol.201, pp.2611-2620, 2006.